

Read the Signs

Towards Invariance to Gradient Descent’s Hyperparameter Initialization

Davood Wadi¹ Marc Fredette¹ Sylvain Senecal²

Abstract

We propose ActiveLR, an optimization meta algorithm that localizes the learning rate, α , and adapts them at each epoch according to whether the gradient at each epoch changes sign or not. This sign-conscious algorithm is aware of whether from the previous step to the current one the update of each parameter has been too large or too small and adjusts the α accordingly. We implement the Active version (ours) of widely used and recently published gradient descent optimizers, namely SGD with momentum, AdamW, RAdam, and AdaBelief. Our experiments on ImageNet, CIFAR-10, WikiText-103, WikiText-2, and PASCAL VOC using different model architectures, such as ResNet and Transformers, show an increase in generalizability and training set fit, and decrease in training time for the Active variants of the tested optimizers. The results also show robustness of the Active variant of these optimizers to different values of the initial learning rate. Furthermore, the detrimental effects of using large mini-batch sizes are mitigated. ActiveLR, thus, alleviates the need for hyper-parameter search for two of the most commonly tuned hyper-parameters that require heavy time and computational costs to pick. We encourage AI researchers and practitioners to use the Active variant of their optimizer of choice for faster training, better generalizability, and reducing carbon footprint of training deep neural networks.

1. Introduction

The current state-of-the-art optimization algorithms are mechanical in their nature, in the sense that they passively

average the gradients, based on a predefined number of past steps, instead of actively adjusting the step size at each epoch according to the change in the sign of the gradients. The moving-average-based optimizers, such as SGD with momentum (Sutskever et al., 2013), Adam (Kingma & Ba, 2014), RAdam (Liu et al., 2019), and RMSprop (Tieleman & Hinton, 2012b), base their optimization calculations on a fixed number of previous gradient values, regardless of what their sign is. If the sign of the gradients changes after epoch e , we want the optimizer to recognize this jump over the optimum immediately and decrease the step size accordingly. Furthermore, current optimizers update all the weights by a global scalar learning rate, α (referred to by most deep learning frameworks as LR or learning rate).

We introduce ActiveLR, an optimization meta algorithm that can be implemented on top of current optimizers to adjust the hyper-parameter α at each epoch for each model parameter. We mathematically prove that ActiveLR variant of a given optimizer has a lower objective function cost compared to the vanilla implementation of that optimizer. One of the main objectives of ActiveLR is to obviate the need for the tuning of the initial learning rate, α , and mini-batch size. For different datasets, architectures, and tasks, the values of α^* , the optimal initial learning rate, and the optimal mini-batch size (Iiduka, 2021), which lead to optimal convergence, are different. Although for well-known benchmark tasks, such as ImageNet with ResNet18 for object recognition, the optimal values for different hyper-parameters have been immensely studied and made publicly available, for new tasks, researchers and practitioners must start anew and perform costly hyper-parameters search to find the optimal values for the initial learning rate, mini-batch size, what learning rate scheduler to use, and at which epochs they should decay the learning rate by what amount.

Moreover, learning rate values higher than α^* lead to divergence of the optimization, while values lower than α^* lead to significantly slower rate of convergence and also increase the possibility of being stuck in a local minimum. Also, large mini-batch sizes are necessary for fast training of large-scale datasets and utilizing the full computational power of multiple GPUs (You et al., 2017). Our tests show that vanilla implementations of SGD with momentum,

¹Department of Decision Science, HEC Montreal, Montreal, QC, Canada ²Department of Marketing, HEC Montreal, Montreal, QC, Canada. Correspondence to: Davood Wadi <davood.wadi@hec.ca>.

AdamW, RAdam, and Adabelief get stuck in local minima for smaller learning rates and fail to achieve high performance on the test set. Moreover, their performance has a negative correlation with mini-batch size. As we increase the mini-batch size, the training becomes unstable and generalizability suffers significantly. On the other hand, ActiveLR implementations of these optimizers (i.e., ActiveSGD, ActiveAdamW, ActiveRAdam, and ActiveBelief) outperform their original implementations, and are also robust to the values of initial learning rate and mini-batch size.

This has major implication for research and practice. Not only is tuning the learning rate and mini-batch size time consuming and costly, it causes severe environmental impacts. For instance, the greenhouse gas emissions for training a state-of-the-art transformers model is equivalent to 10 years of emissions of a person in the U.S. (Lacoste et al., 2019; Strubell et al., 2019). Furthermore, while researchers at large institutions have access to high compute power and afford to perform intense hyper-parameter search on hundreds of GPUs and TPUs, most AI researchers and practitioners have significantly more limited access to computation power. Therefore, ActiveLR helps in democratizing AI, saving time and cost to AI researchers, and also reducing greenhouse emissions.

2. Problemization

SGD and adaptive optimizers have two shortcomings. First, when the optimizer approaches the optimum, the accumulated momentum will cause it to oscillate over the optimum. It is because when the gradient changes its sign, if the exponential moving average has the opposite sign, the weight of the parameter will be updated up the slope of the error curve, deviating the model from the optimum. Therefore, it takes longer for such optimizers to stabilize around the optimum compared to an optimizer that is aware of the gradients’ sign at each step and adjusts the step size, α , according to whether the gradients have changed their sign or not.

Second, using a global learning rate, α , to update all the parameters does not account for the specific position of each neuron compared with its optimum value. At each training epoch, some neurons are farther away from their optimum—requiring a larger α —while others are closer to their optimum—requiring a smaller α . In addition, for a deep neural network, the gradient for middle layers are much smaller compared to the initial and final layers (see 5.1), requiring a larger α . Moreover, when we simultaneously update the weights of a previous layer (e.g. $layer_{i-1}$) to correct the same error function, this simultaneous change in the incoming weights to the next layer ($layer_i$) causes an overshoot effect—determined by the term “fan-in”—on the weights of $layer_i$. The size of fan-in determines the amount of input a layer receives and varies from layer to

layer (Tieleman & Hinton, 2012a). Therefore, we need local α ’s for each neuron to account for these disparities between different neurons.

3. Related work

Jacobs (1988) was the first to suggest that every weight of a neural network be given its own α , and each α be allowed to vary over time. He states that when the sign of the derivative for a parameter is constant for consecutive epochs, the α for that parameter should be increased. On the other hand, when the sign of the derivative for a parameter changes for consecutive epochs, the α for that parameter should be decreased (Figure 1).

Efforts have been made to reduce the sensitivity of gradient descent optimization to learning rate initialization (Baydin et al., 2017; Zhang et al., 2019). However, previous work on reducing sensitivity to initial learning rate has introduced additional hyper-parameters that need to be tuned, which seems to defeat the purpose—removing a hyper-parameter and introducing others to be tuned.

To best of our knowledge, there has not been an automatic algorithm that reduces sensitivity to both initial learning rate and mini-batch size.

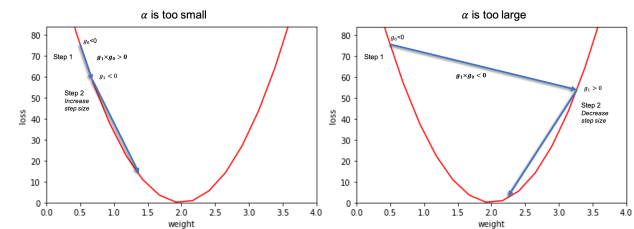


Figure 1. Optimization of a parameter of a model using a sign-conscious optimizer. When the sign of the gradient does not change (left), the Active optimizer increases the step size α , nudging the model weight to the true value of the weight (2.0). When the sign of the gradient changes (right), the weight has jumped over the optimum. Therefore, the Active optimizer decreases the step size α for the next iteration. This not only decreases convergence time, but also avoids constantly jumping over the optimum value.

The latest mention of a sign-conscious optimization algorithm was in (Tieleman & Hinton, 2012a). However, since previous implementations worked only on full-batch training and researchers almost never want to train their neural networks with full batches, the development of sign-conscious optimizers was thwarted.

4. ActiveLR

We introduce a meta algorithm that utilizes a vanilla optimization algorithm, such as Adam or SGD, in the inner-loop part, and in the outer-loop part of the optimization, at every epoch, actively adjusts the local learning rate for each parameter based on the change in the sign of the cumulative gradients. Unlike previous implementations, ActiveLR works with mini-batch and stochastic gradient descent. Almost always, mini-batch gradient descent is the optimal way to train neural networks. Firstly, modern datasets (e.g., ImageNet) do not fit into GPU memory, so full-batch gradient descent on such datasets is not possible. Furthermore, researchers prefer to use mini-batches instead of full-batches, as mini-batches provide faster convergence and better generalizability (Qian & Klabjan, 2020; Wilson & Martinez, 2003).

4.1. The ActiveLR meta algorithm

Assuming we have k mini-batches of data in our dataset, for each iteration t in the dataset, given that each mini-batch of training data has a specific gradient w.r.t. the parameter θ_i , $\nabla f^t(\theta_i^{t-1})$, that is calculated for that mini-batch, we define the cumulative gradient of the model as the arithmetic summation of all mini-batch gradients. For epoch e , the cumulative gradient, ∇f_{cu}^e , with respect to the inner-loop-updated parameter, θ_i , can be derived from:

$$\nabla f_{cu}^e(\theta_i) = \sum_{t=1}^k \nabla f^t(\theta_i^{t-1})$$

The cumulative gradient $\nabla f_{cu}^e(\theta_i)$ is the gradient of the objective function f with respect to the parameter θ_i at epoch e , as if the model has experienced the whole dataset (full-batch training). Since after seeing each mini-batch the optimizer updates the parameters, the calculated gradients for each mini-batch is different from the gradient of the mini-batch if there was no update (this is what we are trying to approximate). Consequently, we wish to prove that the sign of the gradient for the whole dataset with respect to parameter θ_i when the parameter does not change inside the loop is the same as that of the updated parameter within the loop. Thus, we prove the Theorem 1 that enables us to use gradient-descent-updated gradients instead of no-update gradients.

Theorem 4.1. *In the local convex regime of a non-convex objective function, the cumulative gradient of parameter θ_i at epoch e with no inner-loop updates, \widehat{cu} , has the same sign as the cumulative gradient of parameter θ_i at epoch e with inner-loop updates, \widehat{cu} , if the learning rate, α , is smaller than α^* that causes the inner-loop to diverge.*

$$\widehat{cu} \geq 0$$

Algorithm 1 ActiveLR for SGD (ActiveSGD)

Inputs: α^0 {initial learning rate}, θ_i^0 {initial parameter i }, $f(\theta)$ {stochastic objective function}, α_{high} { α growth constant}, α_{low} { α shrink constant}
Output: θ_i^T {the updated parameter i }
 $e \leftarrow 0$, $g_{i,cu}^0 \leftarrow 0$ {initialization}
repeat
 $e \leftarrow e + 1$ {next epoch}
 $t \leftarrow 0$
 $g_{i,cu}^e \leftarrow 0$ {set/reset the cumulative gradient to zero at each epoch}
 for mini-batches in dataset **do**
 $t \leftarrow t + 1$
 $g_i^t \leftarrow \nabla_{\theta_i} f^t(\theta_i^{t-1})$ {calculate the gradient of the objective w.r.t. the parameter at timestep t }
 $g_{i,cu}^e \leftarrow g_{i,cu}^e + g_i^t$ {add mini-batch gradient to cumulative gradient}
 $\theta_i^t \leftarrow \theta_i^{t-1} - \alpha_i^t g_i^t$ {SGD update}
 end for
 $\alpha_i^e \leftarrow \begin{cases} \alpha_i^{e-1} + \alpha_{high}, & \text{sign}(g_{i,cu}^e \times g_{i,cu}^{e-1}) > 0 \\ \alpha_i^{e-1} \times \alpha_{low}, & \text{sign}(g_{i,cu}^e \times g_{i,cu}^{e-1}) \leq 0 \end{cases}$
 {adjust learning rate}
until θ_i^t converged
Return: θ_i^T

ActiveLR can now be implemented using mini-batches by comparing the sign of the cumulative gradient at epoch $e - 1$, $\nabla f_{cu}^{e-1}(\theta_i)$, with the sign of the cumulative gradient at epoch e , $\nabla f_{cu}^e(\theta_i)$ (Algorithm 1). It allows the optimizer to update the parameters at each step of the mini-batch (Wilson & Martinez, 2003; Qian & Klabjan, 2020), while adjusting the α at the end of each epoch (Tieleman & Hinton, 2012a), enabling inner-loop learning through the backend optimizer (e.g., Adam, SGD) and active learning rate adjustment together.

4.2. Orthogonality of ActiveLR to other optimizers

A major advantage of ActiveLR is the orthogonality of the hyper-parameter that it adjusts, α , to the hyper-parameters that other well-known algorithms adjust. To be more specific, we take a look at the generic parameter update that is the backbone of SGD, Adam, RAdam, etc.

$$\theta_i^t \leftarrow \theta_i^{t-1} - \alpha F(g_i^t) \quad (1)$$

The difference among these algorithms is the way they manipulate the $F(g_i^t)$ term through the F function, while keeping α as is in the original SGD algorithm. For instance,

in the case of Adam, $F(g_i^t)$ is $\frac{\beta_1 m_i^{t-1} + (1 - \beta_1) g_i^t}{1 - \beta_1^t}$. However, since ActiveLR modifies the α term in Equation 1, it

can be combined with other optimization algorithms. In fact, in our experiments we report results on ActiveLR combined with SGD with momentum (ActiveSGD), AdamW (ActiveAdamW), with RAdam (ActiveRAdam), and AdaBelief (ActiveBelief) and compare the Active results with their original, vanilla variants.

5. Convergence analysis

At any given epoch, e , we are faced with the choice between the ActiveLR algorithm vs. its corresponding vanilla backbone. We prove that the value of the objective function for ActiveSGD (ActiveLR combined with SGD) at epoch $e + 1$ is as good or better than the vanilla SGD (backbone) algorithm at epoch $e + 1$, and show the conditions where each inequality holds. The proof is capable of any first-order backbone algorithm. For other backbones, such as Adam, RMSProp, etc., their respective ActiveLR implementation should have the same lines of proof, with some modifications peculiar to the optimizer of interest.

Theorem 5.1. *Let us call the cost of vanilla SGD at epoch e , $f(\theta_e^S)$, and the cost of its corresponding ActiveLR implementation, $f(\theta_e^A)$. We define ActiveSGD’s gradient, g_{e+1}^A , as $\frac{\partial f(\theta_e^A)}{\partial \theta_e^A}$, and vanilla SGD’s gradient, g_{e+1}^S , as $\frac{\partial f(\theta_e^S)}{\partial \theta_e^S}$. α is the initial learning rate for ActiveSGD and also the constant learning rate for SGD. α_{High} is the higher learning rate ($\alpha_{High} > \alpha$) that ActiveLR uses when $g_e^A g_{e+1}^A > 0$ and α_{Low} the lower learning rate ($\alpha_{Low} < \alpha$) that ActiveLR uses when $g_e^A g_{e+1}^A < 0$. In the local convex regime of f , at any arbitrary epoch, e , the difference between the cost of using vanilla SGD and ActiveSGD at the next epoch, $e + 1$, is*

$$\begin{cases} f(\theta_{e+1}^S) - f(\theta_{e+1}^A) \geq g_{e+2}^A g_{e+1}^A (\alpha_{High} - \alpha), \\ \text{if } g_e^A g_{e+1}^A > 0. \\ f(\theta_{e+1}^S) - f(\theta_{e+1}^A) \geq g_{e+2}^A g_{e+1}^A (\alpha_{Low} - \alpha), \\ \text{if } g_e^A g_{e+1}^A < 0. \end{cases} \quad (2)$$

where the right hand side for both cases is non-negative.

In other words, ActiveSGD is at least as good as vanilla SGD when gradients are zero (equality in 2), and strictly better than vanilla SGD when gradients are not zero (inequality in 2). The lower bound of the advantage is $g_{e+2}^A g_{e+1}^A (\alpha_{High} - \alpha)$, when $g_e^A g_{e+1}^A > 0$ and $g_{e+2}^A g_{e+1}^A (\alpha_{Low} - \alpha)$ when $g_e^A g_{e+1}^A < 0$.

The hyper-parameters of ActiveLR To set the operations for α_{low} and α_{high} , we follow (Tieleman & Hinton, 2012a)—multiply by α_{low} and add α_{high} . We carry out an ablation analysis of the choice of operations (e.g., addition or multiplication). For the results, please refer to A.3. To

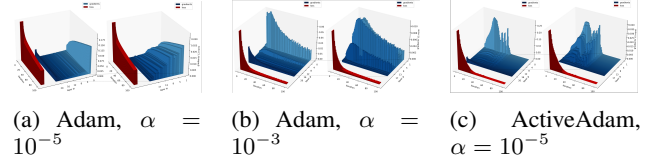


Figure 2. **Gradient norms across layers for CIFAR-10 on ResNet-18.** Vanilla Adam when the α is too small ($\alpha = 10^{-5}$) gets stuck in a local minimum **a**. Vanilla Adam when the learning rate is optimal ($\alpha = 10^{-3}$) oscillates around the optimum **b**. ActiveAdam with the same low learning rate that gets vanilla Adam stuck ($\alpha = 10^{-5}$) achieves minimal loss and remains in the optimum **c**.

obtain the default values of α_{low} and α_{high} , we carry out a preliminary experiment on CIFAR-10 and find that any combination of α_{low} and α_{high} that satisfy the constraint $\alpha_{low} + \alpha_{high} = 1$ reduce sensitivity to initial learning rates and mini-batch size, while increasing the overall accuracy. For all the experiments that follow, we have kept $\alpha_{low} = 0.9$ and $\alpha_{high} = 0.1$ constant. The results show the robustness of the default values of α_{low} and α_{high} across datasets and tasks, which suggests that ActiveLR’s hyper-parameters do not need to be tuned.

5.1. Distribution of gradient norms across layers

We examine the L1-norm of the gradients across layers for the optimization of the CIFAR-10 dataset on the ResNet-18 architecture, which has 21 2D-convolution layers and 1 final fully connected layer (Figure 2). The gradient norm of the final dense layer (layer # = 22) directly correlates with the loss. In contrast, to achieve minimal loss, the gradient norm of the convolutional layers (layer # $\in [1, 21]$) increases to a maximum value (the learning phase) and then decreases (the stabilizing phase around the optimum). For vanilla Adam, when the α is too small ($\alpha = 10^{-5}$), the gradient norm for every convolutional layer increases monotonically with the number of iterations and the loss reaches a plateau, indicating getting stuck in a local minimum **(a)**. In other words, when the learning rate is lower than an optimum value, the learning phase never ends. When the learning rate is optimal ($\alpha = 10^{-3}$), Adam increases the gradient norms to an optimal level where it achieves the minimal loss (the end of the learning phase). Afterwards, in the stabilizing phase, the gradients are decreased at a relatively slow rate, which causes the loss to oscillate (*iteration* > 60) around the minimum value **(b)**. ActiveAdam, with the same low learning rate that gets Adam stuck ($\alpha = 10^{-5}$), is able to achieve what Adam with the optimal learning rate does in the training phase (i.e., increase the gradient norms to a maximum value). Additionally, after the minimal loss is achieved, ActiveAdam sharply reduces the gradient norms, preventing fluctuations around the optimum (*iteration* >

60) (c).

5.2. ActiveLR and non-convex functions

The Active implementation of a given algorithm such as Adam (ActiveAdam) provides numerous advantages over the vanilla implementation in troublesome non-convex optimization scenarios.

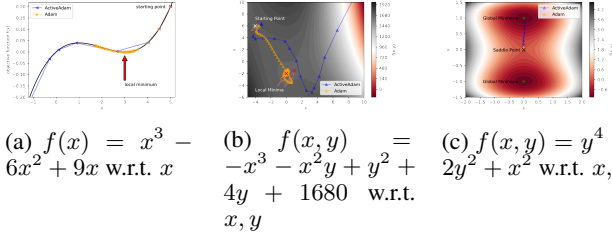


Figure 3. (a) univariate unimodal, (b) bivariate multimodal, and (c) saddle function optimization using vanilla Adam and ActiveAdam

ActiveLR and local minima Local minima are a major plague in deep neural network optimization (Ding et al., 2019; Yun et al., 2018). They are one of the main reasons that optimizers do not generalize well and fail to fit the training data properly. This is especially the case when the learning rate is smaller than an optimum value. In Figure 3a, the vanilla Adam quickly goes down the objective function at the starting point $x = 5$, but as soon as it reaches the local minimum, $x = 3$, the gradient becomes significantly small, causing vanilla Adam to oscillate around the local minimum no matter how long we keep training. ActiveAdam, on the other hand, quickly increases the learning rate, as soon as it realizes that the gradient signs are not changing. It enables ActiveAdam to pass through the local minimum and move towards the global minimum, $x \rightarrow -\infty$. In Figure 3b, the vanilla optimizer faces two challenges. This bivariate function, $f(x, y) = -x^3 - x^2y + y^2 + 4y + 1680$, has three local minima and a global minimum of $(+\infty, +\infty)$. The first local minimum, $(-4, 6)$, the starting point, has a higher function value than the other two, $(0, -2)$ and $(1, -\frac{3}{2})$, which have the same lower value. The first challenge is starting near a local minimum, where the gradients are too small. Adam struggles to escape the starting point because of the small gradients. After a large number of iterations, Adam eventually escapes the starting local optimum but faces the second challenge. It gets trapped in another local minimum, $(0, -2)$, and is unable to escape. ActiveAdam, on the other hand, quickly escapes the initial local minimum since it increases its learning rate when the gradients do not change. With the higher learning rate it has accumulated, it is able to quickly escape the other two local minima and converge to the global minimum, $(+\infty, +\infty)$.

ActiveLR and saddle points Saddle points are another major pitfall in training neural networks (Kawaguchi, 2016). For deep neural networks, large sets of strict and non-strict saddle points have been shown to exist (Achour et al., 2021). Being close to a saddle point equates very small gradient values in all directions. As a result, non-Active optimizers will require significantly higher training iterations to escape saddle points. In Figure 3c, the saddle point lies at $(0, 0)$. After 12 iterations, Adam is relatively where it was when the training started. ActiveAdam, however, quickly increases its learning rate, following iterations of no sign change, and reaches the global minimum at $(0, 1)$ in 12 iterations.

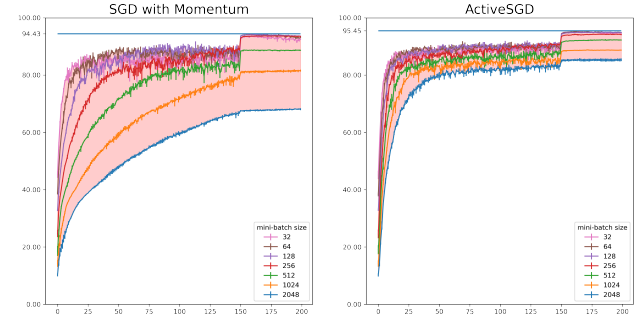


Figure 4. Reduced sensitivity to mini-batch size on CIFAR-10 test accuracy ($[\mu \pm \sigma]$)

6. Experiments

We perform our experiments on ImageNet (Deng et al., 2009) with ResNet-18 and CIFAR-10 (Krizhevsky et al., 2009) with ResNet-34 for image classification, WikiText-2 and WikiText-103 (Merity et al., 2016) with GPT-2 (Radford et al., 2019) for language modelling, and PASCAL VOC (Everingham et al., 2010) dataset on Faster-RCNN+FPN for object detection. Based on the literature, non-adaptive optimizers (e.g. SGD) work with higher initial learning rates compared to adaptive optimizers. Therefore, for all the experiments, we use 50 times the hyperparameter space for initial learning rates of SGD with momentum and ActiveSGD compared to the adaptive optimizers. For each vanilla optimizer and its Active variant, we test the performance across a range of initial learning rates and, for other hyperparameters, we use the values suggested on the optimizer’s official GitHub page for each task. We use a heterogeneous cluster with each node comprised of 4 x NVIDIA P100 Pascal (12G or 16G HBM2 memory) or 4 x NVIDIA V100 Volta (32G HBM2 memory). To simulate common practitioners’ limited access to GPUs, we train the WikiText-2, WikiText-103, PASCAL VOC, and CIFAR-10 experiments on 1 GPU and the ImageNet experiments on 4 GPUs.

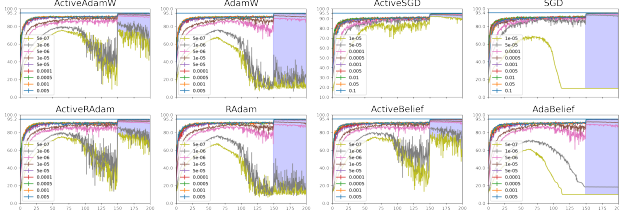


Figure 5. Test accuracy ($[\mu \pm \sigma]$) of SGD with momentum, AdaBelief, RAdam, and AdamW compared with their Active variant on CIFAR-10. The red area in-between lines indicates the sensitivity of the optimizer w.r.t. the value of the initial learning rate. The horizontal lines indicate the highest mean accuracy of each optimizer across learning rates.

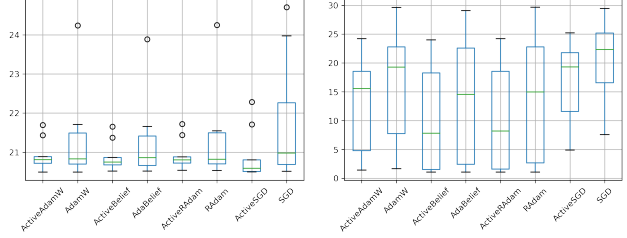
6.1. Sensitivity to mini-batch size

ActiveLR alleviates the problem of large mini-batch sizes by its automatic learning rate adaptation. In Figure 4, we can see that for the CIFAR-10 dataset, increasing the mini-batch size from the optimal value of 128 to larger values significantly decreases the test-set accuracy of vanilla SGD with momentum. Larger mini-batch sizes also destabilize training as can be seen by higher fluctuations in accuracy for vanilla SGD with momentum. ActiveSGD, on the other hand, achieves a relatively high accuracy regardless of the mini-batch size and also remains stable. ($\alpha = 10^{-4}$, ResNet-18)

6.2. Sensitivity to learning rate

CIFAR-10 We train SGD with momentum, AdaBelief, RAdam, and AdamW along with their Active variant (i.e., ActiveSGD, ActiveBelief, ActiveRadam, ActiveAdamW) with 9 different initial learning rates 5×10^n , $n \in [-7, -3]$, each ran 3 times. We test different values for weight decay in the range of $[10^3, 10^{-8}]$ and found that the optimal weight decay, wd^* depends on the learning rate, α . For CIFAR-10, $wd^* \times \alpha = 10^{-4}$. As seen in Figure 5, the Active variant of each optimizer achieves a higher average accuracy compared with the vanilla variant. More importantly, the area between the accuracy achieved by the worst-performing learning rate and the best-performing learning rate is significantly smaller for the Active variants compared to the vanilla variants. This indicates reduced sensitivity to the selection of the initial learning rate that ActiveLR achieves.

WikiText-2 We fine-tune GPT-2 with 124,439,808 parameters on WikiText-2 (vocabulary size 50257, maximum sequence length 1024, dimensionality of the embeddings and hidden states 768, number of hidden layers in the Transformer encoder 12, number of attention heads for each attention layer 12, activation function *gelu*, dropout probabil-



(a) Test-set PPL (lower is better) (b) Train-set PPL (lower is better).

Figure 6. WikiText-2 on GPT-2 with various initial learning rates

ity 0.1). Initial learning rates in the range of $[10^{-8}, 10^{-4}]$ for adaptive optimizers and $[5 \times 10^{-7}, 5 \times 10^{-3}]$ for non-adaptive optimizers are tested. For each initial learning rate, we calculate the test-set PPL for the epoch that gives the highest validation-set PPL. In Figure 6, we can see that ActiveLR gives better test-set PPL compared to vanilla optimizers on average, while producing lower train-set errors. Furthermore, vanilla optimizers have a significant degree of variation in their test-set and train-set PPLs, indicating their sensitivity to the initial learning rate, while ActiveLR shows relative insensitivity to the initial learning rate. A surprising finding is the generalizability of ActiveSGD. Although in the literature the performance of SGD with momentum for transformers models has been shown to be inferior to adaptive methods—and our results confirm it—the ActiveLR variant of SGD with momentum shows better generalizability than the adaptive methods. In fact, ActiveSGD gives the best test PPL among all optimizers tested.

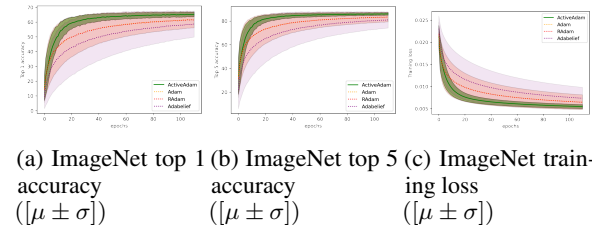


Figure 7. The mean/std test accuracy ($[\mu \pm \sigma]$) of ActiveAdam, AdaBelief, RAdam, and Adam on ImageNet with three initial learning rates ($[10^{-5}, 10^{-4}, 10^{-3}]$). The shaded area around each line is the standard deviation of the means for each optimizer across different values of the initial learning rate. (Adam and RAdam plots are *visually identical*)

ImageNet For ImageNet, we train ActiveAdam, AdaBelief, RAdam, and Adam for 110 epochs, after which the accuracies do not improve. Figure 7 shows the average and standard deviation of each metric across initial learning rates of 10^n , $n \in \{-3, -4, -5\}$. ActiveAdam achieves the highest mean top-1 and top-5 accuracy and the lowest training error (the green line) compared to the other vanilla optimizers (the plots for Adam and RAdam are *visually*

identical). It also has the lowest amount of variance among the optimizers, showing reduced sensitivity to the initial learning rate.

WikiText-103 and PASCAL VOC Please refer to Appendix A.2.

7. Social impact

ActiveLR makes contributions to several social causes. First, given the growth of the size of datasets and deep learning models, it has become increasingly more difficult for average AI practitioners and researchers to train state-of-the-art models. By reducing sensitivity to hyperparameter initialization, ActiveLR helps in democratizing AI. Second, carbon emissions from training deep neural networks have reached alarming levels. Consider training a new dataset with the size of the ImageNet on a relatively small model, such as ResNet-18. Let us assume the goal is to achieve top-1 accuracy of 55% or higher. Since we a priori do not know what the optimal initial learning rate is, we need to test various initial learning rates. Testing 9 initial learning rates starting from 10^{-4} up to 10^0 , we find that, with SGD with momentum, 7 out of 9 initial learning rates achieve our desired accuracy in 100 epochs, while, with ActiveSGD, 8 out of 9 values reach our desired accuracy (Figure 8). Considering the worst-case, where the suboptimal learning rates are selected first, SGD with momentum, compared with ActiveSGD, requires 13,816,000 TFLOPS extra computation (2200 seconds per epoch, 61.11 hours total). With an average carbon efficiency of 0.432 kgCO₂eq/kWh, using 4 x Tesla V100-SXM2-32GB (TDP of 300W) GPUs (same as our experiments), the excessive CO₂ emissions are estimated to be 7.92 kgCO₂eq. This is equivalent to 3.96 Kgs of extra coal burned. On the other hand, ActiveSGD not only prevents such extra carbon emissions, but also gives higher average accuracy and fit (estimations were conducted using the [MachineLearning Impact calculator](#) presented in [Lacoste et al. \(2019\)](#).) As a result, we believe that ActiveLR is a step towards eliminating the need for hyperparameter search, which helps democratize AI and reduce carbon emissions.

8. Limitations

While we try to include as many experiments on various tasks to show the robustness of the results of ActiveLR, due to time and computational limits, we could not test all benchmark datasets. We are working on releasing test results for COCO dataset ([Lin et al., 2014](#)) for object segmentation, and IWSLT14 DE-EN for neural machine translation on transformers, among others, for ActiveLR. With Active LR, we demonstrated the capability to reduce sensitivity to initial learning rate and mini-batch size. We encourage future

research to identify and tackle optimization sensitivity to *other* hyper-parameters, such as weight decay, in an attempt to streamline neural network optimization, reduce carbon emissions, and training time.

9. Conclusion

In this paper, we show that for all the learning rates tested, the Active variant of SGD with momentum, AdamW, AdaBelief, and RAdam achieves the best fit and highest accuracy. Our tests show robust results for different datasets and model architectures. It did so in a lower number of epochs, which translates to faster training. Moreover, we show that ActiveLR remains stable and does not suffer from loss in generalizability when trained with large mini-batch sizes. As a result, multi-GPU training of large datasets can be sped up with ActiveLR using large mini-batch sizes. The orthogonality of ActiveLR to other optimizers allows it to be implemented on top of them. We also show relative insensitivity of ActiveLR to the values of initial learning rate and mini-batch size. We encourage practitioners to use ActiveLR for their model training to achieve better training/test-set performance in a shorter amount of time, remove the need for tuning the initial learning rate and mini-batch size, and reduce their carbon footprint.

Acknowledgements

The authors would like to thank Compute Canada for its provision of computational resources that made the experiments possible.

References

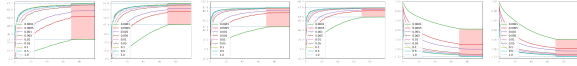
- Achour, E. M., Malgouyres, F., and Gerchinovitz, S. Global minimizers, strict and non-strict saddle points, and implicit regularization for deep linear neural networks. *arXiv preprint arXiv:2107.13289*, 2021.
- Baydin, A. G., Cornish, R., Rubio, D. M., Schmidt, M., and Wood, F. Online learning rate adaptation with hypergradient descent. *arXiv preprint arXiv:1703.04782*, 2017.
- Chen, K., Wang, J., Pang, J., Cao, Y., Xiong, Y., Li, X., Sun, S., Feng, W., Liu, Z., Xu, J., Zhang, Z., Cheng, D., Zhu, C., Cheng, T., Zhao, Q., Li, B., Lu, X., Zhu, R., Wu, Y., Dai, J., Wang, J., Shi, J., Ouyang, W., Loy, C. C., and Lin, D. Mmdetection: Open mmlab detection toolbox and benchmark, 2019. URL <https://arxiv.org/abs/1906.07155>.
- Deng, J., Dong, W., Socher, R., Li, L.-J., Li, K., and Fei-Fei, L. Imagenet: A large-scale hierarchical image database.

- In *2009 IEEE conference on computer vision and pattern recognition*, pp. 248–255. Ieee, 2009.
- Ding, T., Li, D., and Sun, R. Spurious local minima exist for almost all over-parameterized neural networks. *Optimization online*, 2019.
- Everingham, M., Van Gool, L., Williams, C. K. I., Winn, J., and Zisserman, A. The pascal visual object classes (voc) challenge. *International Journal of Computer Vision*, 88(2):303–338, June 2010.
- Iiduka, H. The number of steps needed for nonconvex optimization of a deep learning optimizer is a rational function of batch size. *ArXiv*, abs/2108.11713, 2021.
- Jacobs, R. A. Increased rates of convergence through learning rate adaptation. *Neural networks*, 1(4):295–307, 1988.
- Kawaguchi, K. Deep learning without poor local minima. *arXiv preprint arXiv:1605.07110*, 2016.
- Kingma, D. P. and Ba, J. Adam: A method for stochastic optimization. *arXiv preprint arXiv:1412.6980*, 2014.
- Krizhevsky, A., Hinton, G., et al. Learning multiple layers of features from tiny images. 2009.
- Lacoste, A., Luccioni, A., Schmidt, V., and Dandres, T. Quantifying the carbon emissions of machine learning. *arXiv preprint arXiv:1910.09700*, 2019.
- Lin, T.-Y., Maire, M., Belongie, S., Hays, J., Perona, P., Ramanan, D., Dollár, P., and Zitnick, C. L. Microsoft coco: Common objects in context. In *European conference on computer vision*, pp. 740–755. Springer, 2014.
- Liu, L., Jiang, H., He, P., Chen, W., Liu, X., Gao, J., and Han, J. On the variance of the adaptive learning rate and beyond. *arXiv preprint arXiv:1908.03265*, 2019.
- Merity, S., Xiong, C., Bradbury, J., and Socher, R. Pointer sentinel mixture models. *arXiv preprint arXiv:1609.07843*, 2016.
- Qian, X. and Klabjan, D. The impact of the mini-batch size on the variance of gradients in stochastic gradient descent. *arXiv preprint arXiv:2004.13146*, 2020.
- Radford, A., Wu, J., Child, R., Luan, D., Amodei, D., Sutskever, I., et al. Language models are unsupervised multitask learners. *OpenAI blog*, 1(8):9, 2019.
- Ren, S., He, K., Girshick, R., and Sun, J. Faster r-cnn: Towards real-time object detection with region proposal networks. *Advances in neural information processing systems*, 28, 2015.
- Strubell, E., Ganesh, A., and McCallum, A. Energy and policy considerations for deep learning in nlp. *arXiv preprint arXiv:1906.02243*, 2019.
- Sutskever, I., Martens, J., Dahl, G., and Hinton, G. On the importance of initialization and momentum in deep learning. In *International conference on machine learning*, pp. 1139–1147, 2013.
- Tieleman, T. and Hinton, G. Lecture 6.4 - a separate, adaptive learning rate for each connection. *COURSERA: Neural networks for machine learning*, 4(2):22–25, 2012a.
- Tieleman, T. and Hinton, G. Lecture 6.5-rmsprop: Divide the gradient by a running average of its recent magnitude. *COURSERA: Neural networks for machine learning*, 4(2):26–31, 2012b.
- Wilson, D. R. and Martinez, T. R. The general inefficiency of batch training for gradient descent learning. *Neural networks*, 16(10):1429–1451, 2003.
- You, Y., Gitman, I., and Ginsburg, B. Scaling sgd batch size to 32k for imagenet training. *ArXiv*, abs/1708.03888, 2017.
- Yun, C., Sra, S., and Jadbabaie, A. Small nonlinearities in activation functions create bad local minima in neural networks. *arXiv preprint arXiv:1802.03487*, 2018.
- Zhang, M., Lucas, J., Ba, J., and Hinton, G. E. Lookahead optimizer: k steps forward, 1 step back. *Advances in neural information processing systems*, 32, 2019.
- Zhuang, J., Tang, T., Ding, Y., Tatikonda, S., Dvornek, N., Papademetris, X., and Duncan, J. S. Adabelief optimizer: Adapting stepsizes by the belief in observed gradients. *arXiv preprint arXiv:2010.07468*, 2020.

A. Appendix

A.1. Additional plots

SGD with momentum vs. ActiveSGD for Image-Net on ResNet-18 (Figure 8).



(a) ImageNet top-1 accuracy (b) ImageNet top-5 accuracy (c) ImageNet training loss

Figure 8. The top-1, top-5, and training loss of SGD with momentum and ActiveSGD on ImageNet with 9 initial learning rates $[10^{-4}, 10^0]$. The shaded area shows the performance gap between the best initial learning rate and the worst one (sensitivity to the value of initial learning rate.)

CIFAR-10 training loss on ResNet-34 (Figure 9).

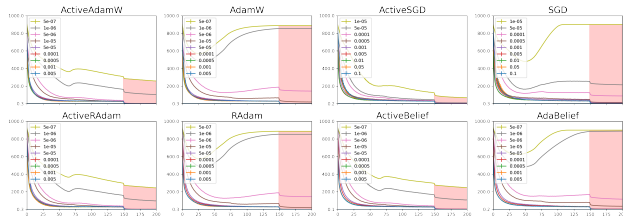


Figure 9. Training loss ($[\mu \pm \sigma]$) of SGD with momentum, AdamW, ActiveSGD, ActiveAdamW, RAdam, and AdaBelief compared with their Active variant on CIFAR-10. The red area in-between lines indicates the sensitivity of the optimizer w.r.t. the value of the initial learning rate. The horizontal lines indicate the lowest loss of each optimizer across learning rates.

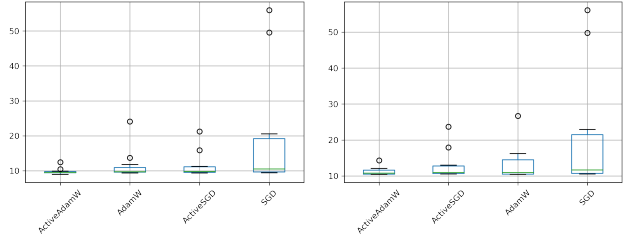
A.2. Extra experiments

WikiText-103 on mini-GPT2 We train WikiText-103 on a small variant of GPT-2—mini-GPT-2 1 from scratch.

Figure 10 shows the test and training PPLs for SGD with momentum, AdamW, ActiveSGD and ActiveAdamW. They show that compared with the vanilla variants, the ActiveLR variants achieve better training fit and test-set PPL. Moreover, lower variance of ActiveSGD and ActiveAdamW PPLs show the reduced sensitivity of the ActiveLR variants to the value of the initial learning rate compared with the vanilla variants.

The training hyperparameters are in Table 2.

PASCAL VOC on Faster-RCNN We train PASCAL VOC on Faster-RCNN (Ren et al., 2015) with pretrained ResNet-50 backbone, following (Zhuang et al., 2020).



(a) Test-set PPL (lower is better) (b) Train-set PPL (lower is better)

Figure 10. WikiText-103 on mini-GPT-2 with various initial learning rates

Table 1. mini-GPT-2 specifications

HYPERPARAMETER	VALUE
VOCABULARY SIZE	10,000
BLOCK SIZE	200
NUMBER OF LAYERS	2
NUMBER OF ATTENTION HEADS	2

The results are shown in Figure 12. Note that we could not replicate the mAP from (Zhuang et al., 2020); we suspect the reason is their use of the MMDetection (Chen et al., 2019) framework, which does various extra image augmentation transforms.

A.3. The choice of α_{low} and α_{high}

We run a simulation to see the range of the learning rate after going through a series of α_{low} and α_{high} updates. We simulate a setting where the learning rate, α , with 0.5 probability, is decreased by α_{low} , otherwise, it is increased by α_{high} . The simulation is run for 10^4 epochs.

In Figure 13 we see that, consistent with (Tieleman & Hinton, 2012a), only multiplying by α_{low} and adding to α_{high} maintain a stable and positive learning rate ($\mu_\alpha = 1.0$, $\sigma_\alpha = 0.3$). Other combinations lead to a negative learning rate (subtract-add and subtract-multiply) or shrink the learning rate to 0 (multiply-multiply).

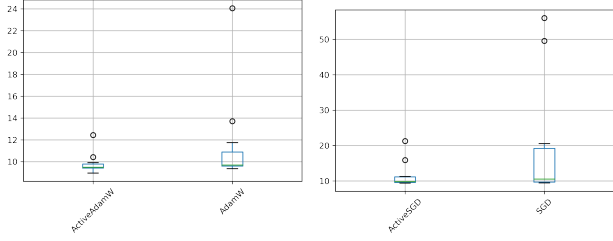
A.4. Proofs

Theorem 4.1 In the local convex regime of a non-convex objective function, the cumulative gradient of parameter θ_i at epoch e with no inner-loop updates, $\hat{c}u$, has the same sign as the cumulative gradient of parameter θ_i at epoch e with inner-loop updates, $\hat{c}u$, if the learning rate, α , is smaller than α^* that causes the inner-loop to diverge.

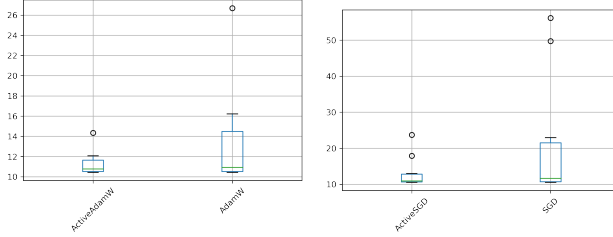
$$\hat{c}u^* \hat{c}u \geq 0 \quad (3)$$

Table 2. WikiText-103 on mini-GPT-2 hyperparameters

HYPERPARAMETER	VALUE
MINI-BATCH SIZE	128
MAXIMUM NUMBER OF EPOCHS	200
WEIGHT DECAY	0.0
NON-ADAPTIVE OPTIMIZERS' LEARNING RATES	$[5 \times 10^{-6}, 10^{-1}]$
ADAPTIVE OPTIMIZERS' LEARNING RATES	$[10^{-7}, 10^{-2}]$



(a) Test-set PPL (lower is better) (b) Test-set PPL (lower is better).

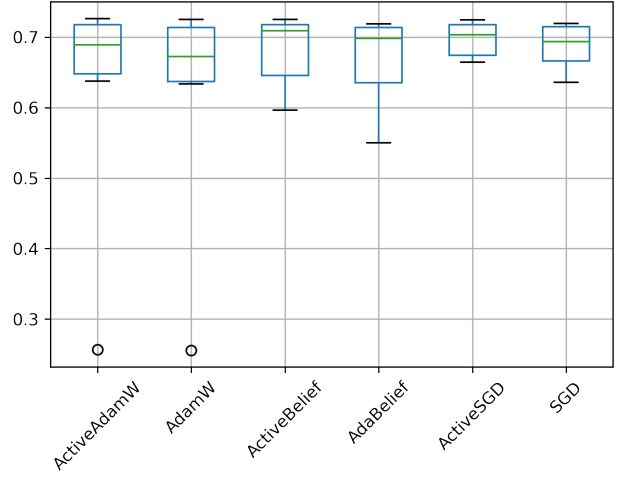


(c) Train-set PPL (lower is better) (d) Train-set PPL (lower is better).

Figure 11. WikiText-103 on mini-GPT-2 with various initial learning rates

Proof. We prove this for the general case of the cost function f for inner-loop updates of SGD. We wish to show that at time K , for a dataset of K mini-batches, the cumulative gradient when there is no inner-loop updates to the parameters, $\hat{c}u$, has the same sign as the cumulative gradient when there is SGD updates at each iteration to the parameters, $\hat{c}u$. Suppose we are optimizing parameters θ using a convex objective function $f(\theta_t, batch_t)$, where θ_t and $batch_t$ are the parameter and the mini-batch at time-step t . For ease of notation, we will refer to the objective function evaluated for $batch_t$ as f_t . We will also refer to the gradients of the objective function w.r.t. the parameter θ_t for mini-batch t , as $g_t(\theta_t)$. When there are no inner-loop updates, we will refer to the parameter as θ_t^* , which will equal the initial θ , i.e., θ_0 , regardless of the value of t . When there are SGD updates in the inner-loop, we will refer to the parameter as $\hat{\theta}_t$, which will be determined by the SGD algorithm 5. Formally,

$$\theta_t^* = \theta_0 \quad (4)$$



(a) Test-set mAP (higher is better)

Figure 12. PASCAL VOC on Faster-RCNN with various initial learning rates

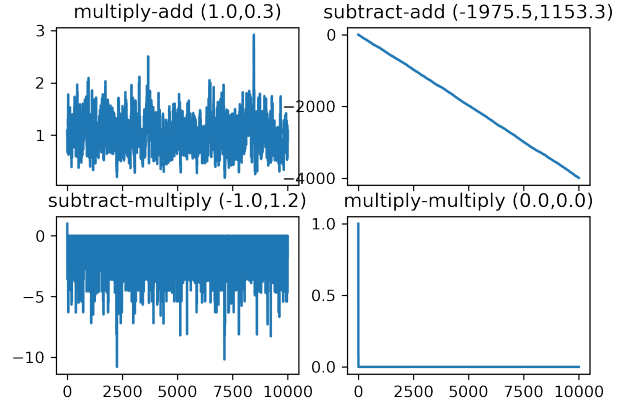


Figure 13. learning rate (y-axis) plotted against training epochs (x-axis)

$$\hat{\theta}_t = \hat{\theta}_{t-1} - \alpha g_t(\hat{\theta}_{t-1}), \quad (5)$$

where α is the constant, positive learning rate and

$$g_t(\theta) = \frac{\partial f_t(\theta)}{\partial \theta} \quad (6)$$

The no-update and SGD-updated cumulative gradients are

defined as follows:

$$\begin{aligned} cu^* &= \sum_{t=1}^K g_t(\theta_{t-1}^*) \\ \widehat{cu} &= \sum_{t=1}^K g_t(\widehat{\theta}_{t-1}) \end{aligned} \quad (7)$$

Since 5 is recursive, we can unroll it from $\widehat{\theta}_{t-1}$ through $\widehat{\theta}_0$:

$$\widehat{\theta}_t = \theta_0 - \alpha \sum_{i=1}^t g_i(\widehat{\theta}_{i-1}) \quad (8)$$

In order to prove the theorem, we will use the following property of convex functions:

Supposing that f is a convex function, a and b two points in the domain of f , and $\frac{\partial f(b)}{\partial b}$ the derivative of f at point b , we have:

$$f(a) - f(b) \geq \frac{\partial f(b)}{\partial b}(a - b) \quad (9)$$

We use 9 on $\widehat{\theta}_K$, i.e., the final parameter after the updates, and θ_0 , the initial parameter, for the objective function evaluated on batch t :

$$f_t(\widehat{\theta}_K) - f_t(\theta_0) \geq \frac{\partial f_t(\theta_0)}{\partial \theta_0}(\widehat{\theta}_K - \theta_0) \quad (10)$$

Replacing $\frac{\partial f_t(\theta_0)}{\partial \theta_0}$ with $g_t(\theta_0)$ according to 6:

$$f_t(\widehat{\theta}_K) - f_t(\theta_0) \geq g_t(\theta_0)(\widehat{\theta}_K - \theta_0) \quad (11)$$

Replacing $\widehat{\theta}_K - \theta_0$ with the unrolled version from 8:

$$f_t(\widehat{\theta}_K) - f_t(\theta_0) \geq -\alpha g_t(\theta_0) \sum_{i=1}^K g_i(\widehat{\theta}_{i-1}) \quad (12)$$

From the theorem's assumption that the optimization does not diverge, it follows that the objective function for the final parameter θ_k should have a lower value than the initial parameter θ_0 :

$$f_t(\widehat{\theta}_K) - f_t(\theta_0) \leq 0 \quad (13)$$

Combining 12 and 13, we have:

$$\begin{aligned} 0 &\geq f_t(\widehat{\theta}_K) - f_t(\theta_0) \geq -\alpha g_t(\theta_0) \sum_{i=1}^K g_i(\widehat{\theta}_{i-1}) \\ 0 &\leq f_t(\theta_0) - f_t(\widehat{\theta}_K) \leq \alpha g_t(\theta_0) \sum_{i=1}^K g_i(\widehat{\theta}_{i-1}) \end{aligned} \quad (14)$$

From 7, we replace $\sum_{i=1}^K g_i(\widehat{\theta}_{i-1})$ with \widehat{cu} :

$$0 \leq f_t(\theta_0) - f_t(\widehat{\theta}_K) \leq \alpha g_t(\theta_0) \widehat{cu} \quad (15)$$

Finally, we sum over all the mini-batches in the dataset, $t=1 \dots K$:

$$\begin{aligned} 0 &\leq \sum_{t=1}^K [f_t(\theta_0) - f_t(\widehat{\theta}_K)] \leq \sum_{t=1}^K [\alpha g_t(\theta_0) \widehat{cu}] \\ 0 &\leq \sum_{t=1}^K [f_t(\theta_0) - f_t(\widehat{\theta}_K)] \leq \alpha \widehat{cu} \sum_{t=1}^K g_t(\theta_0) \end{aligned} \quad (16)$$

From 4 and 7, $\sum_{t=1}^K g_t(\theta_0) = cu^*$:

$$0 \leq \sum_{t=1}^K [f_t(\theta_0) - f_t(\widehat{\theta}_K)] \leq \alpha \widehat{cu} cu^* \quad (17)$$

Since α is positive:

$$0 \leq \frac{\sum_{t=1}^K [f_t(\theta_0) - f_t(\widehat{\theta}_K)]}{\alpha} \leq \widehat{cu} cu^* \quad \square \quad (18)$$

We see that $\widehat{cu} cu^*$ is non-negative and found a lower bound $\frac{\sum_{t=1}^K [f_t(\theta_0) - f_t(\widehat{\theta}_K)]}{\alpha}$ for it. \square

Theorem 5.1 Let us call the cost of vanilla SGD at epoch e , $f(\theta_e^S)$, and the cost of its corresponding ActiveLR implementation, $f(\theta_e^A)$. We define ActiveSGD's gradient, g_{e+1}^A , as $\frac{\partial f(\theta_e^A)}{\partial \theta_e^A}$, and vanilla SGD's gradient, g_{e+1}^S , as $\frac{\partial f(\theta_e^S)}{\partial \theta_e^S}$. α is the initial learning rate for ActiveLR SGD and also the constant learning rate for SGD. α_{High} is the higher learning rate ($\alpha_{High} > \alpha$) that ActiveLR uses when $g_e^A g_{e+1}^A > 0$ and α_{Low} the lower learning rate ($\alpha_{Low} < \alpha$) that ActiveLR uses when $g_e^A g_{e+1}^A < 0$. In the local convex regime of f , at any arbitrary epoch, e , the difference between the cost

of using vanilla SGD and ActiveLR SGD at the next epoch, $e + 1$, is

$$\begin{cases} f(\theta_{e+1}^S) - f(\theta_{e+1}^A) \geq g_{e+2}^A g_{e+1}^A (\alpha_{High} - \alpha), \\ \text{if } g_e^A g_{e+1}^A > 0. \\ f(\theta_{e+1}^S) - f(\theta_{e+1}^A) \geq g_{e+2}^A g_{e+1}^A (\alpha_{Low} - \alpha), \\ \text{if } g_e^A g_{e+1}^A < 0. \end{cases} \quad (19)$$

where the right hand side for both cases is non-negative.

Proof. At the start, the parameters and gradients are equal for ActiveLR and vanilla SGD:

$$\begin{aligned} \theta_e^A &= \theta_e^S \\ g_{e+1}^A &= g_{e+1}^S \end{aligned} \quad (20)$$

θ_{e+1}^A and θ_{e+1}^S are as follows:

$$\theta_{e+1}^S = \theta_e^S - \alpha g_{e+1}^S \quad (21)$$

Replacing θ_e^S with θ_e^A and g_{e+1}^S with g_{e+1}^A ,

$$\theta_{e+1}^S = \theta_e^A - \alpha g_{e+1}^A \quad (22)$$

For ActiveLR,

$$\begin{cases} \theta_{e+1}^A = \theta_e^A - \alpha_{High} g_{e+1}^A, \\ \text{if } g_e^A g_{e+1}^A > 0. \\ \theta_{e+1}^A = \theta_e^A - \alpha_{Low} g_{e+1}^A, \\ \text{if } g_e^A g_{e+1}^A < 0. \end{cases} \quad (23)$$

For a differentiable convex function, f , at two points a and b in its domain, we have

$$f(a) \geq f(b) + \frac{\partial f(b)}{\partial b} (a - b). \quad (24)$$

From 24, for θ_{e+1}^A and θ_{e+1}^S we have

$$f(\theta_{e+1}^S) \geq f(\theta_{e+1}^A) + \frac{\partial f(\theta_{e+1}^A)}{\partial \theta_{e+1}^A} (\theta_{e+1}^S - \theta_{e+1}^A) \quad (25)$$

Replacing $\frac{\partial f(\theta_{e+1}^A)}{\partial \theta_{e+1}^A}$ with g_{e+2}^A

$$f(\theta_{e+1}^S) - f(\theta_{e+1}^A) \geq g_{e+2}^A (\theta_{e+1}^S - \theta_{e+1}^A) \quad (26)$$

Replacing from 22 and 23 into 26:

$$\begin{cases} f(\theta_{e+1}^S) - f(\theta_{e+1}^A) \geq g_{e+2}^A g_{e+1}^A (\alpha_{High} - \alpha), \\ \text{if } g_e^A g_{e+1}^A > 0. \\ f(\theta_{e+1}^S) - f(\theta_{e+1}^A) \geq g_{e+2}^A g_{e+1}^A (\alpha_{Low} - \alpha), \\ \text{if } g_e^A g_{e+1}^A < 0. \end{cases} \quad (27)$$

We can divide the training process into two segments, e_0 to e_{switch} when the gradients change after each epoch, and $e_{switch+1}$ to the end of training, e_T , when the gradients do not change. Note that the opposite can be also be true, i.e., e_0 to e_{switch} is when the gradients do not change after each epoch, and $e_{switch+1}$ to the end of training, e_T , when the gradients change after each epoch. Here we treat the former. After the proof of the former, the latter can be proved trivially.

While we are in the segment e_0 to e_{switch} , since the gradients change sign after each epoch, $g_{e+2}^A g_{e+1}^A < 0$ and $g_e^A g_{e+1}^A < 0$. Therefore, the second inequality of 27 holds. On the right hand side, we have $\alpha_{Low} - \alpha < 0$ from the theorem's assumption. As a result, the right hand side is non-negative, and $f(\theta_{e+1}^S) - f(\theta_{e+1}^A)$ is greater than or equal to a non-negative number.

When we are in the segment $e_{switch+1}$ to e_T , since the gradients do not change sign after each epoch, $g_{e+2}^A g_{e+1}^A > 0$ and $g_e^A g_{e+1}^A > 0$. Therefore, the first inequality of 27 holds. On the right hand side, we have $\alpha_{High} - \alpha > 0$ from the theorem's assumption. As a result, the right hand side is non-negative, and $f(\theta_{e+1}^S) - f(\theta_{e+1}^A)$ is greater than or equal to a non-negative number. \square

A.5. Interactive webapp

We created an interactive webapp where the readers can compare the performance of ActiveAdam and Adam in minimizing a saddle and an MSE loss function, with the ability to change hyper-parameter values, such as initial learning rate, initial weight, and number of epochs. The webapp can be accessed through the link below:

<https://active-lr.herokuapp.com>

B. Notes on the appended codes

The training scripts are written for SLURM workload manager since our experiments were run on HPCs with SLURM.

B.1. License

The licenses for the assets used in this paper are the following:

- AdamW: This work is licensed under a BSD 3-Clause "New" or "Revised" License
- RAdam: This work is licensed under a Apache License 2.0
- AdaBelief: This work is licensed under a BSD 2-Clause "Simplified" License
- CIFAR-10 and -100: This work is licensed under a New BSD License

- WikiText-2 and -103: This work is licensed under a Creative Commons Attribution-ShareAlike License
- ImageNet: This work is licensed under a custom (research, non-commercial) license
- GPT-2: This work is licensed under a Modified MIT License